

A HYBRID 4π DETECTION SYSTEM FOR 100-GeV PHOTON PHYSICS AT NAL

Z. G. T. Guiragossian and F. Villa
Stanford Linear Accelerator Center

ABSTRACT

Utilizing an extensive simulation technique, a five-meter superconducting magnet with a streamer chamber is proposed as a NAL facility for 100-GeV photon physics. The system is extended necessarily by wire spark-chamber planes, e/γ detectors, and a π/K Cerenkov counter. A tagged photon beam study is also made with new yield calculations.

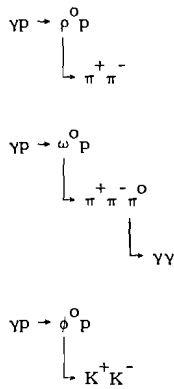
I. INTRODUCTION

In this study we propose a hybrid 4π detection system specifically for 100-GeV photon physics at NAL. It is clear that the proposed system can be extended readily for π/K beam physics in this energy range. The system consists¹ of a 4-5 meter diameter superconducting magnet, a streamer chamber and several wire spark chambers together with neutral detectors and a π/K threshold Cerenkov counter. Its performance has been examined by extensive Monte Carlo simulation of events. The subject of photon physics at NAL has been discussed in previous studies by Heusch,² Wilson,³ and Toner.⁴

The study of photoproduction processes is a necessary complement to the understanding of hadron-hadron interactions in that it supplies a separate method for the investigation of dynamical processes and examines the link between both types of interactions. Current theories of Regge exchange, diffraction scattering, and vector-meson dominance are directly influenced by such a joint understanding of photoproduction processes and hadron-hadron interactions. At NAL, for the first time, appreciably useful photon and electron beams will be available at high-energy proton accelerators so that photoproduction and electroproduction programs can be supported as well as hadron physics programs at the same facilities.

Specifically, we propose a detection system for the study of the following processes:

1. Vector meson photoproduction as a function of k_γ .



2. Search for massive vector particles.
3. Measurement of the total hadronic γp cross section, $\sigma_{\text{tot}}(\gamma p)$, as a function of k_γ .
4. Measurement of the Compton scattering cross section, $\sigma_{\text{el}}(\gamma p)$, as a function of k_γ .
5. The A-dependence of processes 1-4 by the measurement of the above, photo-produced on complex nuclei: Be, C, Al, Cu, Ag, and Pb.
6. The 4π detection ability should make such a system to be attractive as well for the study of electromagnetic processes with selective triggers.

It is clear that particular detection systems can be designed for the specific study of any one of the above experiments. These have been discussed by others. Here, we propose a general detection system for the above experiments, where modifications can be made in a modular fashion for specific studies of varying complexity.

II. BEAM

The preparation of a tagged photon beam for NAL was studied by Heusch,² Wilson,³ and Toner.⁴ We have re-examined these studies and summarize here our choice of parameters for such a beam. Also, an independent yield calculation is made based on the multiperipheral model of Chew and Pignotti⁵ which reaffirms the results obtained by the statistical thermodynamics model of Hagedorn and Ranft.^{6,7}

Figure 1(a) shows the forward differential distribution in the cross section of π^+ , π^- , and π^0 production from 200-GeV pp collisions as computed from the multiperipheral model. The π^0 yield is approximated by the average of π^+ and π^- productions. For computational purposes the π^0 yield is parametrized by a fourth order polynomial (open circles).

The most efficient primary production target T should be a material of low Z and small ratio λ_c/X_0 of collision to radiation length. For practical reasons this is chosen to be 40 cm of Be. This corresponds to $1/3 \lambda_c$ and attenuates $\leq 20\%$ of the primary photons from $\pi^0 \rightarrow \gamma\gamma$ decays, by e^+e^- pair production. A clearing magnet sweeps all charged particles away from the first radiator R_1 . For efficient electron conversion, R_1 should be a material of highest Z and largest λ_c/X_0 ratio. It can be shown⁴ that if R_1 is more than $(0.2-0.3) X_0$ in thickness, then this becomes an inefficient radiator which depletes the high-energy components in the electron spectrum due to thick radiator straggling effects. For this purpose, R_1 is chosen to be 1.5 mm of Pb. Figure 1(b) gives the forward π^0 yield from the primary target T, the primary photon spectrum from T, and the electron yield at R_1 . The spectral integration procedures are indicated on this figure.

The processes which enter in the preparation of a tagged photon beam ($\pi^0 \rightarrow \gamma\gamma$, $\gamma \rightarrow e^+e^-$, $e^- \rightarrow e^- \gamma$) have small characteristic angles ($\theta_\gamma^\pi = m_{\pi^0}/E_{\pi^0}$, $\theta_{em} = m_e/E_e$). The typical transverse momentum due to these is ~ 100 MeV/c. In view of this, the beam transport design can be made, from the primary π^0 to the final tagged photon, as if we had a charged pion beam. Figure 2 summarizes the schematic layout for such a beam. Electrons are chosen over positrons because of the higher abundance of positively charged hadrons produced at R_1 due to the large neutron background in the primary photon beam. We note that hadron production here proceeds with transverse momenta 3 or 4 times larger than in the electromagnetic processes. For this reason, a dispersion-free image of the primary target is required so that most of the hadrons can be collimated out of R_2 , the thin tagging radiator. This focused and achromatic electron beam is reimaged on the final beam monitor, a quantameter. Such refocusing allows for the detection and separation of forward photons produced at the experimental detector's target. R_2 is a $0.02-0.05 X_0$ high-Z radiator. A beam profile of $1-2 \text{ cm}^2$ is expected. The photon tagging method is well known; we choose a tagging counter bank of twenty $1\% \Delta E/E$ intervals.

III. EXPERIMENTAL TARGETS

Considerations of the experimental detector target size include the following conditions: 1) ability to reconstruct interaction vertices as accurately as possible, 2) ability to detect a given minimum recoil proton momentum, and 3) ability to maintain a constant level of background for a fixed experimental arrangement. The first condition, together with the expected pencil-like photon beam profile, determines transverse dimensions not exceeding 2×2 cm. Since our targets are placed inside a magnet, in the cases of hydrogen and deuterium the requirement of maximal track length within the magnetic field dictates a target length as short as possible. If, in

addition, we choose a value of 150 MeV/c for the minimum detectable recoil proton momentum, then the use of high pressure gas targets for hydrogen and deuterium is favored over liquid targets. Finally, condition (3) requires that all targets be made of equal radiation length. The target materials of interest are hydrogen, deuterium, Be, C, Al, Cu, Ag, and Pb. For hydrogen and deuterium we choose high pressure gas targets (~500 psi) with dimensions of $2 \times 2 \times 30$ cm. Such targets are currently being constructed at SLAC with fiberglass containers.

IV. EXPERIMENTAL DETECTION SYSTEM

Hybrid experimental detection systems are a natural consequence of high-energy accelerators. As beam energy increases more $\int Bdl$ is required to measure momenta and longer lever arms for accurate angular definitions. General purpose large devices tend to be unyielding to modifications from experiment to experiment. They are expensive both in construction and operation. As a result of these, hybrid detector systems for hadron physics at NAL have been considered by T. Fields et al.,⁸ A. Roberts and T. G. Walker,⁹ and W. D. Walker.¹⁰ Here, a small hydrogen bubble chamber is used for vertex definition and event recognition followed by large spectrometers and optical spark chambers. On the basis of data reduction ease, R Hulsizer¹¹ proposed to substitute a streamer chamber in place of a bubble chamber for the above hybrid systems.

Design Criteria

We have designed a hybrid system specifically for photon physics at NAL. Some of the criteria that enter into such a design are the following:

1. Ability to detect signals unambiguously from the processes under investigation, over backgrounds which are about 150 times larger than these. e^+e^- pair production is 150 times larger than hadron photoproduction. Such a large background does not exist in hadron physics experiments.
2. Provision of visual guidance for event definition at a minimal cost.
3. High accuracy in event reconstruction.
4. Discrimination against a large background level demands a fast triggering ability together with a good device memory and a rapid cycling capacity.
5. At these energies, the highly forward collimation of events requires a large lever arm for accurate angular definition of tracks.
6. The proper identification of chosen reactions requires the ability to detect externally the presence of charged and neutral kaons and event-associated neutrals (whether these are forward γ 's or a peripheral neutron).
7. A general data-reduction method is needed which can be applied to the entire experimental program.

8. The detector configuration should be suitable for both standard and automatic data-reduction facilities.

9. Finally, manageable detector-system dimensions enter in the very important considerations of fabrication cost, device installation, and operation.

The above criteria are by no means exhaustive. However, we think that at least these should be considered in any first-order estimation.

Final Configuration

Among several configurations investigated by Monte Carlo simulation of events, we present that which conforms best to our criteria. Figure 3 displays schematically the entire detector layout. A 5-meter diameter, 20-kG superconducting magnet with a 1-meter gap contains a streamer chamber with dimensions of $5 \times 2 \times 1$ meters. The magnet allows for a three-view photography system 8 meters above the beam line. The incident photon beam is convergent, focused onto the final γ beam detector. Forward charged pions are distinguished from kaons in symmetrical, four-segment, 4.5-meter long, 40×40 cm threshold Cerenkov counters. Five sets of wire spark-chamber planes (modules) of 2×4 meters dimension are positioned at 3-meter intervals behind the magnet. One-meter long shower counter wings are placed on both sides of the wire spark chambers to detect the presence of lower energy electrons. At the end are located the high-energy electron, γ and hadronic particle discrimination arrangement, and the γ beam veto and monitoring quantimeter. The magnet is surrounded by neutral particle detectors. The major components of this arrangement are now discussed.

V. HYBRID SYSTEM COMPONENTS

A. Magnet

Clearly, this is the costliest item in the system and, for this reason, it requires a careful analysis. Our complete-event simulation studies have convinced us that for 100-GeV physics, this 100 kG-m magnet is sufficient for accurate event reconstruction in the hybrid system. However, our computer simulation was done assuming a uniform field strength. Briefly, 60 kG-m hurt the physics, 80 kG-m can be considered adequate. For this reason our proposal is based on a 100 kG-m inhomogeneous magnet, since an accurate field map of better than 0.2% for a magnet of this size would be impractical to expect. This magnet could conceivably be air core superconducting coils with some superconducting mirrors or additional iron. Field inhomogeneity of ~50% around the forward beam envelope as seen in Fig. 3 can be tolerated adequately. Event reconstruction programs with helical trajectory integration routines have been in operation at SLAC. As compared with bubble-chamber homogeneous magnets, the trajectory integration reconstruction program operates a

factor of 5-10 times slower. This can be compensated by the decreasing cost per cycle time on the developing new computers. We believe that a 5-meter diameter 20-kG air core superconducting magnet, with some 50% inhomogeneity around a defined envelope can be constructed at less cost than homogeneous field magnets and can perform adequately for accurate event reconstruction in 100-GeV physics experiments.

B. Threshold Cerenkov Counters

The design of this system is based on the expected charged pion and kaon momentum vs transverse exit coordinate distributions. These have been obtained through our simulation studies (see below). The counters are segmented to sample several ranges. This Cerenkov counter is used to improve the distinction between events containing charged π 's and K's. Tentatively, this will be 4.5 meters long and operating at atmospheric pressure. The inner center sections cover a transverse dimension of ± 40 cm. Each counter here has transverse dimensions of 40×40 cm, filled with He gas at STP, giving Cerenkov light of 4.5 photons/meter (threshold $\gamma = 119$). The two outer sections, 40 cm wide upbeam and 60 cm wide downbeam, will be filled with Ne gas at NTP, giving 12 photons/meter (threshold of $\gamma = 85$). Parabolic mirrors focus the Cerenkov light onto 9-inch photomultipliers positioned above the beam plane.

C. Wire Spark Chambers

The five sets of wire spark-chamber modules, as seen in Fig. 3, are a necessary and integral part of this hybrid detector system. They serve to define a large lever arm for the charged tracks and thus to increase their angular definition. In actuality, since the magnet is expected to have a highly inhomogeneous field, these wire spark chambers will also be useful for a more accurate momentum determination, provided that a good field map is made. (In practice, the trajectory integration will be carried outside the magnet with increasingly larger step sizes.) The first four modules have one meter long shower counter wings added on each side, with vertical dimension 10 cm. These are positioned at the beam plane and serve to indicate the presence of lower energy electrons which come from photoabsorption by the e^+e^- pair production process. The last set of planes, WSC5, can be used strictly for reaction-induced photon identification and angular definition. Our simulation studies show that this module is highly efficient for the detection of $\pi^0 \rightarrow \gamma\gamma$ in the reaction of $\gamma p \rightarrow \omega^0 p$ (see Fig. 5). Also, our simulation studies show that sufficient dimensions for the wire spark chambers with this magnet are 2×4 meters.

In our configuration, each WSC module is actually made up of pairs of xx-yy-uu-vv planes, with 0, 90, 30, and 120 degree orientations respectively. The

chambers are made with 1 mm wire spacing, and within each pair of planes only the wires of one plane are used actively for readout. A small on-line computer of PDP-15 type is used to collect data from these chambers along with monitoring all of the counter information.

Considering the size of these chambers and the neighborhood of an inhomogeneous magnetic field, we have considered a recent development in wire spark-chamber technology which is based on field emission transistor (FET), individual wire readouts. The advantages in such a system are 1) practically unlimited memory time, 2) each wire pair acts independently of its neighbor, thus the number of sparks that can be sustained is not a limitation, 3) the chambers are insensitive to the presence of magnetic fields, 4) and an accuracy of 500μ in space is obtained, as in other such systems, for track coordinate definition.

D. Neutral Detectors

An integral part of our triggering system is the ability to detect the presence of reaction-produced photons together with a knowledge of the maximum number of reaction-associated photons. The position of WSC5 and the open area surrounding the magnet gap are used for this purpose.

E. Trigger System

Our trigger system should 1) identify the presence of a tagged photon at the experimental target, 2) exclude the large electromagnetic background, primarily from e^+e^- pair production, and 3) inhibit the presence of large numbers of reaction-associated neutrals. Because of the high duty cycle and good time resolution at hand, we let the e^+e^- pairs go through the entire detection system. To demonstrate feasibility let us assume a tagged photon beam at 5×10^4 equivalent quanta/pulse with a $0.03X_0$ experimental target. This gives 1,500 e^+e^- pairs/pulse. The streamer chamber has a memory time $\leq 10 \mu\text{sec}$ and a trigger logic with 10 nsec time resolution can be expected. The probability that a hadronic event will be lost because such an event and a pair occur at the same time interval is

$$\frac{1,500 e^+e^-/\text{pulse} \times 10^{-8} \text{ sec}}{0.50 \text{ sec/pulse}} = 3 \times 10^{-5}.$$

The probability that a hadronic event and an e^+e^- pair shall be found together in the streamer chamber is

$$\frac{1,500 e^+e^-/\text{pulse} \times 10^{-5} \text{ sec}}{0.50 \text{ sec/pulse}} = 0.03.$$

Thus, 3% of the streamer-chamber pictures will contain a e^+e^- pair and a hadronic event. The presence of pairs is recognized by the scintillator, lead, WSC5, and shower counter hodoscope arrangement and the 1-meter long shower-counter wings of the first four wire spark-chamber modules.

The streamer chamber and the wire spark chambers will be triggered by a signal with the following logical components:

<u>Objective</u>	<u>Logic</u>	<u>Reason</u>
1% $\Delta E/E$ electron beam hitting the radiator R_2	yes	} γ beam and energy proper identification
Tagged electron, one and only one	yes	
Guard against trident and other second order e/γ processes	no	
Streamer chamber charged particle guard counter	no	
One charged particle on the hodoscope in front of the last wire spark chamber and/or other SC surrounding counters	yes	outgoing hadrons
Large pulse height from WSC(1-4)-wing shower counters or behind WSC5 shower counter, initiated by a charged particle	no	No e^+e^- pairs produced
Pulse from the γ beam detector behind WSC5	no	beam γ absorption
All other guard counters	no	background rejection

VI. EVENT SIMULATION

A complete Monte Carlo simulation of events has been performed upon vector meson photoproduction processes at 100 GeV. The following design parameters are input to the programs:

1. A photon beam of 100 GeV with 1% $\pm\Delta E/E$ resolution.
2. A 5-meter diameter, 1-meter gap, 20-kG uniform field magnet.
3. A 5-meter long, 2-meter wide and 1-meter high streamer chamber.
4. A 30-cm long, 1x1 cm cross section, high-pressure hydrogen gas target.

We define the origin of our space-coordinate system to be located at the beginning of the magnet and situated at the center, transversely and vertically. Let x be the beam direction, y transverse, and z vertical directions. The target is placed between $x = 15$ to 45 cm and the five wire spark-chamber modules at $x = 8, 11, 14, 17,$ and 20 m.

A three-view camera system is assumed for the streamer-chamber photography, with maximum off-axis viewing angle of 25° . The camera plane is located at $z = 8$ meters with (x,y) coordinates of $(3, 1)$, $(3, -1)$, and $(1.25, 0)$ meters. The streamer chamber is photographed with a demagnification of 80, using 35 mm perforated film with 25 mm useful width. The lenses have a 9.875 cm focal length and the lens nodal plane to film plane distance is 10 cm. We have assumed a space reconstruction uncertainty derived from an 8-micron film-plane error, which includes both measuring errors and residual optical distortions.

By Monte Carlo simulation, tracks are generated in space as they would appear to come from the vector meson photoproduction processes. That is, the vector mesons are produced with a known momentum transfer dependence of e^{-At} , have a decay distribution in their own rest frame of $\sin^2 \theta$ and have a Breit-Wigner resonant shape with known masses and widths. Event vertices are chosen randomly within the above target volume. With this definition, tracks are generated within the streamer chamber, trajectories integrated within the specified magnet and, whenever possible, continued to intersect the wire spark-chamber planes. With the known track trajectories for a given event, space coordinate points are generated every 30 cm if the track segment is inside the streamer chamber (every 10 cm if the momentum is less than 1 GeV/c) and at the wire spark chamber hit positions.

Since a measurer will not be able to distinguish between two small-opening forward tracks near the target, we deleted generated film points in the beginning of any forward track if its other neighbor had a transverse separation of less than 4 mm in space.

In this manner we have generated 200 random events for ρ^0 , ω^0 , and ϕ^0 photoproduction reactions. Figures 4(a), 4(b), and 5(a) show the charged particle hit plots for the three reactions at the last wire spark chamber (WSC5). Figure 5(b) shows the $\pi^0 \rightarrow \gamma\gamma$ hit plot from ω^0 photoproduction. It is seen that with very high efficiency the presence of associated photons can be detected. We stress that these chambers' usefulness for charged tracks lies in determining the angular definition of forward tracks.

Figures 6(a) and (b) show the momentum vs transverse displacement of π^+/K^+ tracks. This information is used to design the threshold Cerenkov counters situated immediately behind the magnet. These distributions are obtained at a position 3 m behind the magnet.

To test the detection efficiency and resolution of this system, these events, in Monte Carlo generated film plane data form, were processed by the space-reconstruction and kinematical fitting programs SYBIL and TEUTA and tested for several reaction hypotheses. Track mass assignments were permuted to examine

false fits, 4c and 1c category fits were done, altogether for nine hypotheses, on all the "events." We find that based upon kinematical fits alone, 90% of all the events are truly identifiable. A very good criterion in this identification is the computed mass of the beam particle. Our beam was assumed to have an energy uncertainty of $\pm 1\%$ and angular uncertainty of 2 mrad. All "false" mass permutation fits gave photon masses in the GeV range, true constraints had $-0.3 \leq m_{\gamma}^2 \leq +0.3 \text{ GeV}^2$.

Figure 7 shows the $\pi^+ \pi^- \pi^0$ effective mass distribution obtained after reconstruction and kinematical fit of $\gamma p \rightarrow \omega^0 p$ events. From this we conclude that ± 10 -MeV mass resolution is expected from our system, which is adequate for physics purposes. If need be, a factor of two improvement can be obtained readily by using 70 mm film. The choice of 35 mm film is due to economic reasons and we feel that the achievable accuracy is much better than the one used in this simulation study.

VII. STREAMER CHAMBER AND MODULATORS

The streamer chamber proposed here has a gap which is slightly larger than the present SLAC chamber. The existing high-voltage modulators driving the SLAC streamer chamber will be adequate for our purposes. That is, a specific technical development is not necessary and existing designs can be scaled up. Other current improvements,¹² specifically for the removal of flares, will be incorporated in the final design of such a system. Hence, we do not foresee the necessity of any further technical development to implement our proposal.

Data Rate

We expect a maximum of 5×10^4 tagged equivalent quanta/pulse. Assuming a 30-cm long liquid hydrogen target and a $\sigma_{\text{tot}}(\gamma p) \approx 100 \text{ } \mu\text{barn}$ for total hadronic photoproduction cross section. Previous experience from SLAC photoproduction experiments in the streamer chamber leads to an expected trigger rate of 5 triggers/sec. This rate can be handled with existing streamer-chamber cameras and no new technical developments are needed. Under actual conditions we believe the data rate will be about 1 good event/sec.

VIII. COST ESTIMATE

The 5-meter superconducting magnet cost estimate is based on initial calculations by H. Brechna (SLAC). Figure 8 shows the initial estimated dimensions of the superconducting coils and iron yoke. The magnet's top opening is required for the streamer chamber's viewing purposes. This design of the coils and yoke is made to compensate for the top opening and to give a 20-kG field with 20% inhomogeneity over ± 2.5 meters.

Superconducting Magnet Cost Estimate.

Coils and iron	1,300,000
500 W refrigerator	300,000
Installations	100,000
Auxiliary	<u>100,000</u>
Subtotal	\$ 1,800,000

Other System Components:

3 cameras (with 2 spares) data board, vacuum loops, and control electronics	150,000
1 million volt modulator and streamer chamber power supply	160,000
Streamer chamber	100,000
Wire spark chambers	350,000
WSC modulators, electronics and readout	300,000
Building and utilities (at \$50/ft ²)	500,000
Counters	100,000
Computer with on-line data reduction capability	<u>500,000</u>
	\$ 2,160,000
Tagged photon beam facility	<u>400,000</u>
Total	\$ 4,360,000

IX. CONCLUSION

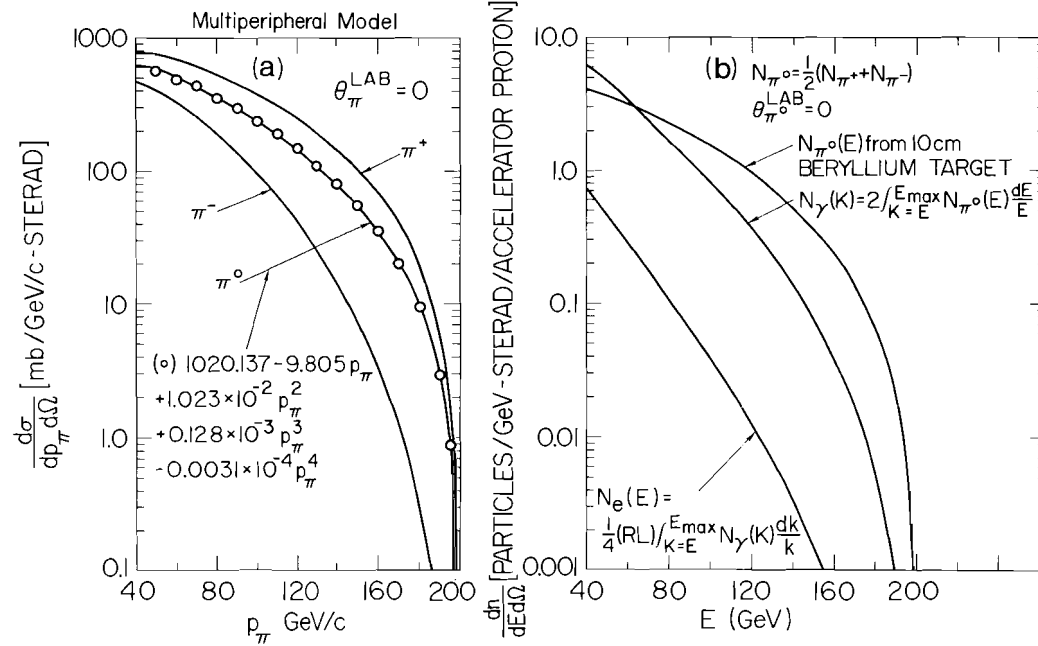
We have designed a 4π hybrid detection system for accurate photoproduction studies in the 100-GeV range. Our simulation studies show that with such a system, once a signal's presence is detected, it can be resolved with reliability and accuracy.

REFERENCES

¹This combination of detectors for a 4π hybrid system was first examined by A. I. Alikhanian (Yerevan) and Z. G. T. Guiragossian (SLAC) in their Proposal for a 10-50 GeV Photon Beam at Serpukhov and Photoproduction Experiments Using a System of Streamer Chamber and Wire Chambers (1969).

- ²C. A. Heusch, Lawrence Radiation Laboratory Report UCRL-16820, Vol. III, p. 156, 1967; An Electron-Photon Facility for the National Accelerator Laboratory, National Accelerator Laboratory 1968 Summer Study Report B. 9-68-109, Vol. II, p. 163.
- ³R. Wilson, Electromagnetic Physics at NAL, National Accelerator Laboratory 1968 Summer Study Report B. 9-68-49, Vol. II, p. 135.
- ⁴W. T. Toner, Electron and Photon Beams at NAL, National Accelerator Laboratory 1968 Summer Study Report B. 9-68-31, Vol. II, p. 125; Design of an Experiment to Measure σ_{TOT} ($\gamma p \rightarrow$ Hadrons) at Very High Energies, National Accelerator Laboratory 1968 Summer Study Report B. 9-68-40, Vol. II, p. 189; Problems in Attempting to Measure $d\sigma/dt$ ($\gamma p \rightarrow \gamma p$) Compton Scattering, National Accelerator Laboratory 1968 Summer Study Report B. 9-68-48, Vol. II, p. 197.
- ⁵G. F. Chew and A. Pignotti, A Simple Formula for the Distribution of Energetic Secondary Baryons From Proton-Initiated Collisions, National Accelerator Laboratory 1968 Summer Study Report E-68-53, Vol. III, p. 324; L. Caneschi and A. Pignotti, Phys. Rev. Letters 22, 1219 (1969). We thank Dr. Pignotti for several illuminating discussions and for supplying a computational program.
- ⁶R. Hagedorn and J. Ranft, Suppl. Nuovo Cimento 6, 169 (1968).
- ⁷T. G. Walker, Secondary-Particle Yields at 200 GeV, National Accelerator Laboratory 1968 Summer Study Report B. 5-68-24, Vol. II, p. 59.
- ⁸T. Fields, A. Roberts, D. Sinclair, J. VanderVelde, and T. G. Walker, A Hybrid Detector System for 100-GeV Strong Interactions, National Accelerator Laboratory 1968 Summer Study Report A. 3-68-12 (Revision), Vol. III, p. 227.
- ⁹A. Roberts and T. G. Walker, Further Studies on a Combined Bubble-Spark Chamber High-Accuracy Detection System for Multiparticle Final States at 100 GeV/c, National Accelerator Laboratory 1968 Summer Study Report A. 3-68-13, Vol. III, p. 237.
- ¹⁰W. D. Walker, On the Use of a Hybrid Bubble Chamber in the 100-BeV Region, National Accelerator Laboratory 1968 Summer Study Report A. 3-68-100, Vol. III, p. 299.
- ¹¹R. Hulsizer, Comments on Substituting a Streamer Chamber for the Bubble Chamber in the Hybrid Bubble-Chamber-Spark Chamber Detector Proposed By Fields et al., National Accelerator Laboratory 1968 Summer Study Report A. 3-68-95, Vol. III, p. 274.
- ¹²F. Villa, What Is New in Streamer Chambers, National Accelerator Laboratory 1969 Summer Study Report SS-60, Vol. III.

200 GeV PROTONS-NATIONAL ACCELERATOR LABORATORY



- 305 -

Fig. 1(a). Forward pion-production differential cross section from 200-GeV pp interactions computed from a multi-peripheral model (Ref. 5). The π^0 yield is approximated by the average of π^+ and π^- productions. (b) The forward π^0 yield from a 10 cm Be target and the resulting primary γ spectrum from 200-GeV pp collisions. The electron yield is obtained from 0.25 X_0 Pb converter.

- 13 -

SS-76

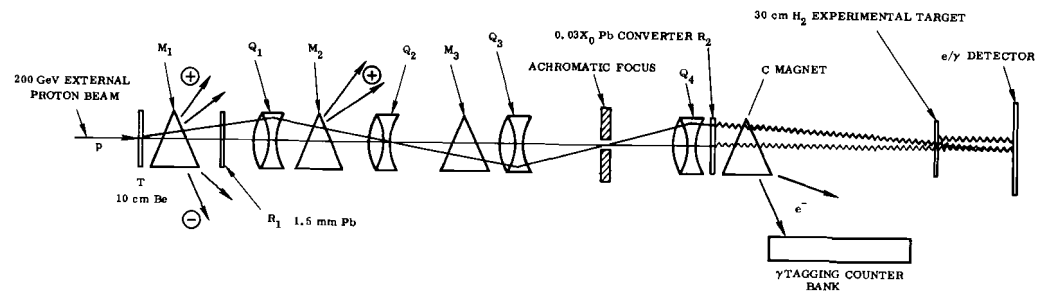


Fig. 2. Tagged γ -beam schematic layout and preparation of an achromatic 100-GeV electron source.

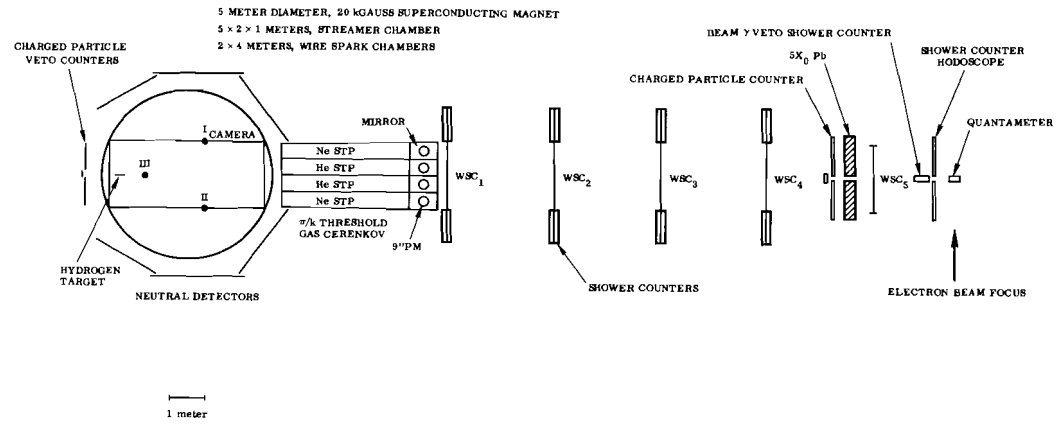


Fig. 3. Proposed hybrid experimental detection system.

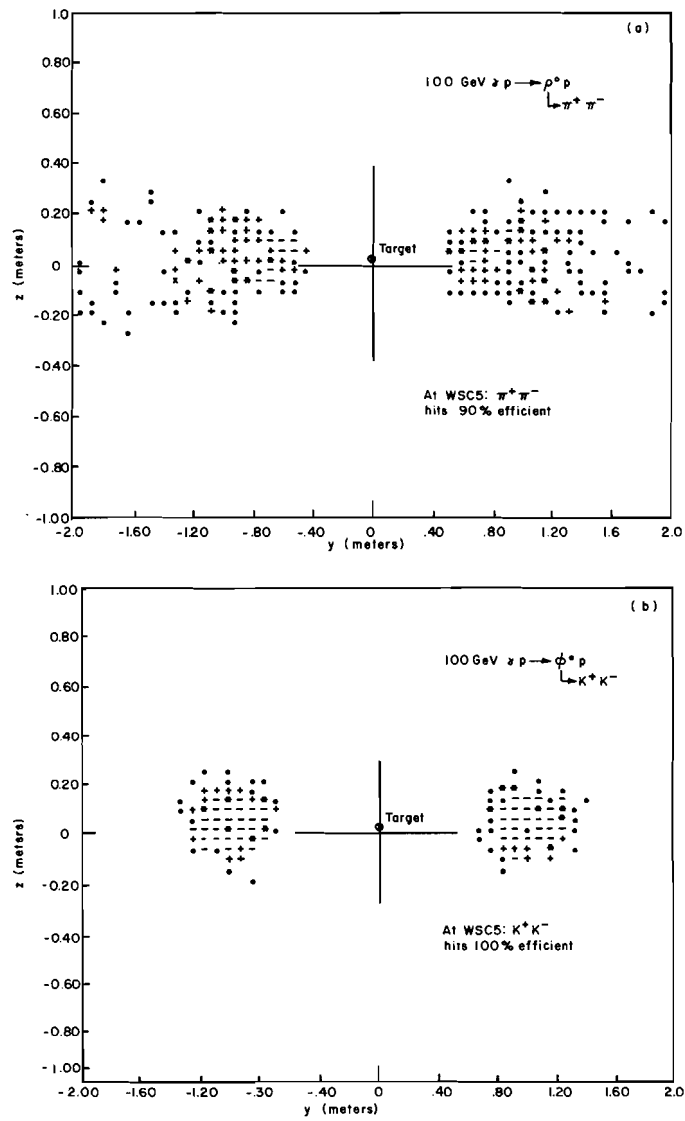


Fig. 4. Track coordinate plots of hits at the last wire spark-chamber module from (a) ρ^0 photoproduction and (b) ϕ photoproduction. Hit symbols are (·) one hit, (+) two hits, (*) three hits, (-) four or more hits at specified locations.

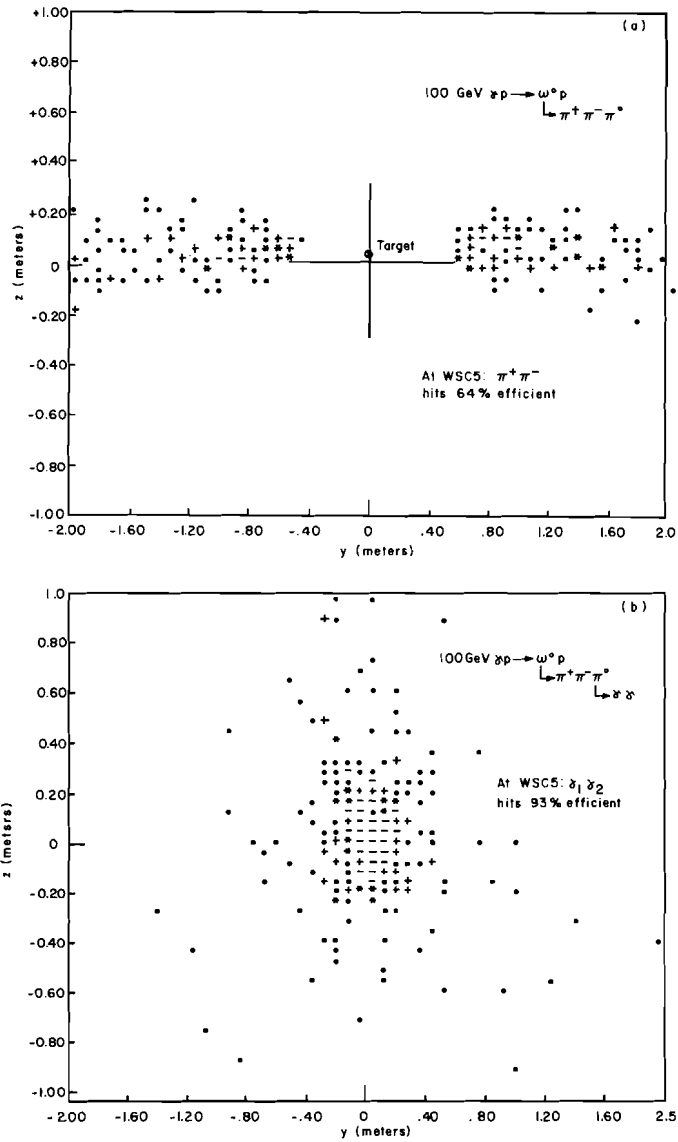


Fig. 5. Track coordinate plots of hits at the last wire spark-chamber module from $\gamma p \rightarrow \omega^0 p$ Monte Carlo generated events. (a) for charged pions, and (b) for $\pi^0 \rightarrow \gamma\gamma$.

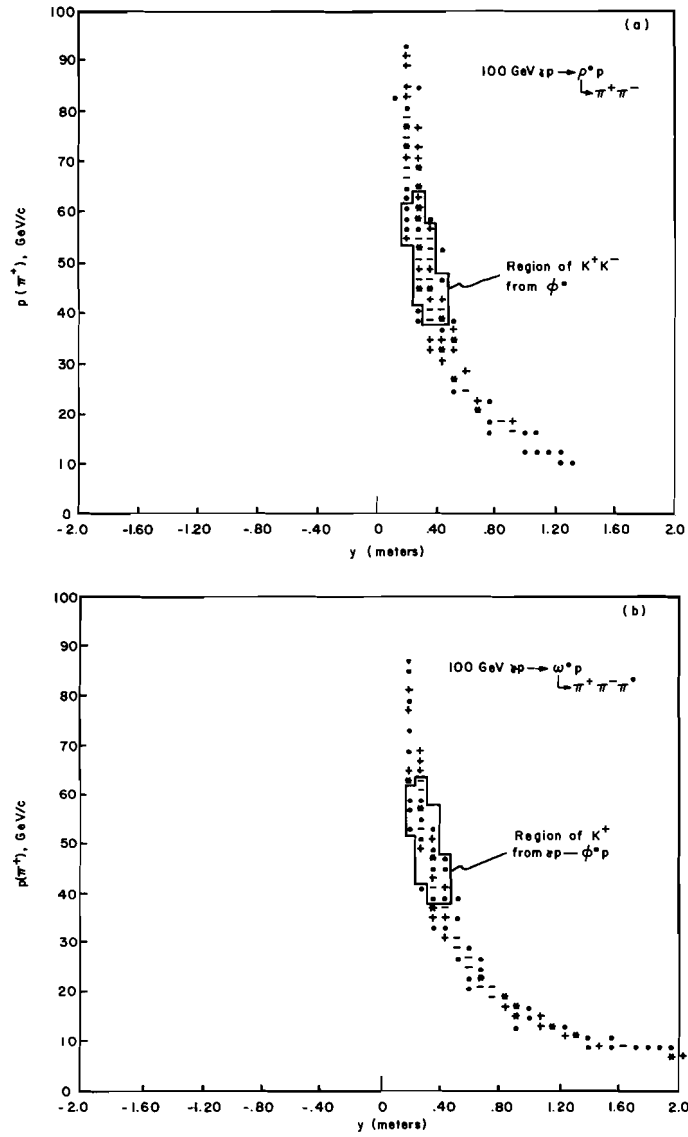


Fig. 6. π^+ / K^+ momentum distribution vs transverse displacement of tracks at the Cerenkov counters. The inserts are for K^+ from ϕ^0 photoproduction.

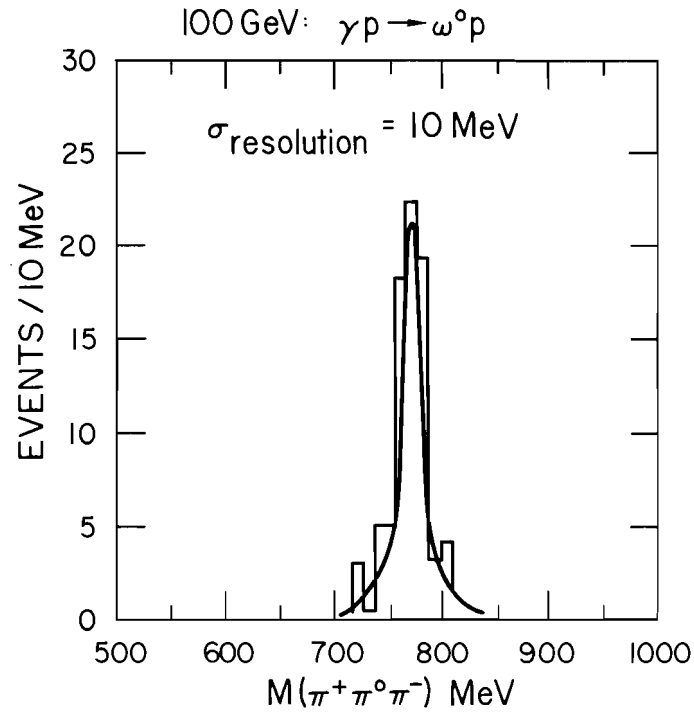


Fig. 7. Effective mass distribution $M(\pi^+ \pi^0 \pi^-)$ from simulated ω^0 photoproduction events, after reconstruction and kinematic fits.

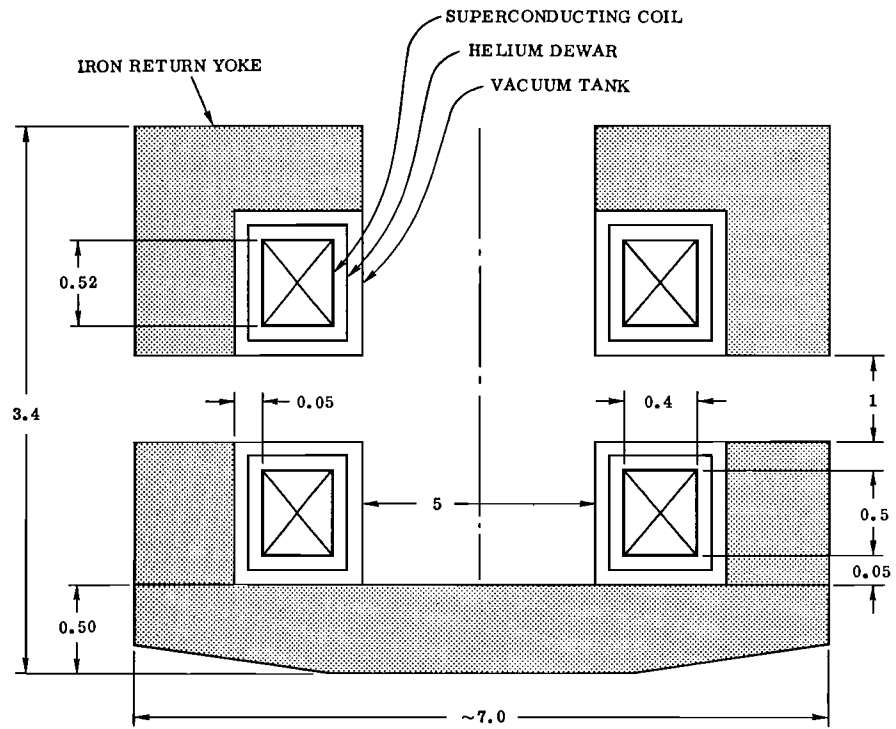


Fig. 8. Five-meter diameter, 20-kG superconducting magnet. Dimensions in meters.